NOVEL FLAW CLASSIFICATION AND PROFILING ALGORITHM USING DATA FUSION OF MULTIFREQUENCY EDDY CURRENT MEASUREMENTS FROM AIRCRAFT STRUCTURES

SUBMITTED BY:

MOEZ UL HASSAN

SUPERVISED BY:

CDR DR TARIQ MAIRAJ RASOOL KHAN PN

Thesis Submitted in Partial Fulfillment of the requirements for the Degree of

Master of Science in Electrical Engineering with Specialization in

Control Systems

at Department of Electronics & Power Engineering

Pakistan Navy Engineering College, Karachi

National University of Sciences & Technology, Islamabad, Pakistan

October, 2014

National University of Sciences & Technology, Pakistan Navy Engineering College, Karachi

Title of Thesis:

Novel Flaw Classification and Profiling Algorithm using Data Fusion of Multifrequency Eddy Current Measurements from Aircraft Structures

Submitted By:

Name: Moez ul Hassan

Reg No.: 2011-NUST-MS-PHD-ELEC (Con-N)-14

Discipline /Deptt: MS Control/EPE

Supervised by:

Cdr. Dr. Tariq Mairaj Rasool Khan PN

Assistant Professor

Guidance and Examination Committee:

1. Cdr. Dr. Faisal Amir PN

   Assistant Professor
2. Dr. Muhammad Bilal Kadri

   Assistant Professor
3. Cdr. Dr. Sajid Saleem PN

   Assistant Professor

TABLE OF CONTENTS

LIST OF FIGURES

LIST OF TABLES

ACKNOWLEDGEMENT

In the name of Allah, the Most Gracious and the Most Merciful

All praises to Allah for the strengths and His blessing in completing this thesis. Foremost, I would like to express my deep gratitude to my thesis supervisor Cdr. Dr. Tariq Mairaj Rasool Khan for his continuous guidance and enthusiastic encouragement for the completion of this thesis. I would also like to thanks the members of the committee Cdr. Dr. Faisal Amir, Dr. Muhammad Bilal Kadri and Cdr. Dr. Sajid Saleem, for their advice and assistance in keeping my progress on schedule.

I would like to take this opportunity to thank PNEC, NDT Research Centre team and ICT R&D for their help in offering me the resources in running the research work. My grateful thanks are also extended to Pakistan International Airline NDT team for providing support in site measurements. Sincere thanks to my friend M. Noman Khan for their kindness and moral support during my thesis.

Finally, and most importantly, I would like to thank my parents, brother and sister for their unwavering support during my study. My pursuit of a MS would not have been possible without them.

ABSTRACT

Aerospace nondestructive testing (NDT) is performed to determine the structural integrity of aircraft structure. It is mandatory for safety of passenger and aircraft that periodic testing of aircraft structures must be carried out for damages such as corrosion and cracks. Currently aircrafts Non Destructive Testing (NDT) is performed at Pakistan according to OEM's instructions. NDT signal measurements are sent to aircraft manufacturers in writings, who then examine the results and suggest the subsequent corrective action.

The purpose of this research is to perform multi frequency eddy current nondestructive evaluation (NDE) on aerospace structures to determine their structural integrity. During the conduct of this research, Eddy current testing data is acquire from NDT facilities of Pakistan International Airlines by scanning structures composed of electrically conductive materials at different scan frequencies. Modern signal processing algorithm is develop to improve signal to noise ratio of the NDT measurement data. Advanced adaptive thresholding algorithm is also applied to obtain potential region of interest from actual NDT data into. The regions of interest (ROI) detected after preprocessing scheme contains discriminatory features. The features extracted from ROIs in Eddy Testing data include amplitude and phase in single frequencies and multiple frequencies, phase trend (increase or decrease in phase of signal with respect to frequencies), flaw length etc. On the basis of extracted features, rules base algorithms develop which classify defected areas from non-defect regions. Once the flaw/damage is detected, statistical as well as deterministic algorithms is implemented to quantify this inverse problem. Modern data fusion technique is incorporated in profiling algorithm to improve the accuracy of the solution.

Reliable data fusion methods in the field of eddy current nondestructive evaluation are required to increase accuracy and reduce uncertainty. Therefore, a novel technique presented in this thesis reformulated the renowned spatial temporal correlation method as spatial frequency correlation method to handle multi frequency eddy current data fusion problem. The proposed method is applied on corrosion quantification problem of aging aerospace structures to investigate the efficacy of the method. The data set includes eddy current testing results from aircraft lap joint attained at four different frequencies. The final fused image through spatial frequency correlation method is further compared with corresponding true digital x-ray thickness map for hidden corrosion.

The proposed classification algorithms reduce the number false calls and results in relatively small number of regions that need to be analyzed by the classification algorithm. The promising result of characterization and corrosion quantification presented in the thesis also indicates the efficacy of the proposed data fusion technique.

The major conclusion of the project is improvement in aerospace NDT infrastructure in Pakistan. If a component failure is incorrectly diagnosed one or many times, that clearly represents an increased requirement for maintenance human resources as well as facilities. A related factor that often is not considered is the wear that occurs as a result of multiple repair attempts. Not only are components damaged as a result of un-necessarily replacement but additional wear and costs are incurred.

CHAPTER 1

1 INTRODUCTION

1.1 Non Destructive Testing

New demands on machinery have stimulated the development and use of new materials whose operating characteristics are not completely known. These new materials when used in critical areas like aircraft parts could create potentially dangerous problems. Therefore, sufficient and proper NDT tests can save many lives. Non Destructive testing (NDT) methods are defined to test the material without harming its future usefulness [1]. It is used to inspect especially the material integrity or properties of the test object. Non Destructive testing methods has been classified into six major categories depending upon the material and type of defect detection [2]. The objective of each method is to provide information about discontinuities, structure thickness, mechanical properties and composition of the test object. Evaluation of conductive materials such as copper, aluminum or steel; eddy current testing is the obvious choice [3].

1.2 Aerospace Non Destructive Testing

Aging aircraft structures are prone to corrosion, which weaken the damage tolerance capability and accelerate the growth of cracks within the structure [4]. Aerospace nondestructive testing (NDT) is performed to determine the structural integrity of aircraft structure. The major components of the aircraft structure inspected include fuselage, wings, stabilizers, appendages, lap joints, multi layered structures etc. Modern aircraft maintenance management organizations have been undertaking projects to improve diagnostics, prognostics and enhanced supply chain integration for a very long time. These initiatives have improved the safety of aircrafts as well as

made flight operations commercially viable. Modern algorithms are being implemented for damage diagnostics and prognostics in aerospace industry. The existing solution approaches to diagnosis can be divided into two broad categories. Direct methods rely on the use of signal processing techniques to establish a relationship between specific characteristics of the signal and the geometry of the defect, ignoring the underlying physical process. These methods typically pose the inverse problem as determining a mapping from the measurement space to the material property space [3-4] where the set of unknown parameters that define the mapping are determined from measurements. Direct approaches ranging from calibration methods to more recent procedures based on neural networks [5-6] have all been proposed. The advantages of this approach are their simplicity and speed; however, the approaches are also very sensitive to the analytical models that are used as well as noise in the measurements. Phenomenological methods usually rely on a physical model to accurately simulate the underlying physical phenomenon and predict the probe response [7]. The model is used to estimate the measurement given the flaw profile, which is iteratively derived by minimizing the difference between the estimated and actual measurements. Minimization may be through conventional techniques such as conjugate gradient, though other techniques such as simulated annealing [8] or genetic algorithms [9] have also been proposed. Eddy current NDT are often used to test aerospace structures to detect damage incurred in service.

1.3 Eddy Current Non Destructive Testing

Electromagnetic testing (ET) since 1880 has evolved from relatively simple devices to metal characterization [10]. In 1868, a British engineering publication reported that discontinuities were being located in gun barrels by using a magnetic compass to register the flux [11]. Later

after World War II, these techniques of signal analysis on the complex plane became widely used in analysis of eddy current tests following their clear enunciation by Friedrich Foster [12].

Innumerable examples of Eddy Current tests have been reported in the literature and in patents. Many provided eddy current coils into which round bars or other test objects were placed producing simple changes in amplitudes of test signals or unbalanced simple bridge circuits [13, 14, 15].

The basic principle underlying eddy current inspection methods can be illustrated with a simple arrangement shown in Figure 1-1. When a coil carrying an alternating current is brought in close proximity to an electrically conducting material, an alternating magnetic field is established as per Amperes Law. This magnetic field causes currents to be induced in the conducting test specimen in accordance with Faraday's law of electromagnetic induction. The induced currents are called eddy currents since they follow closed circulatory patterns that are similar to eddies found in water bodies. The alternating eddy current, in turn, establishes a field whose direction is opposite to that of the original or primary field in accordance with the Lenz's Law. Consequently, the net flux linkages associated with the coil decreases. Since the inductance L of a coil is defined as the number of flux linkages $\forall$ per ampere I, the effective inductance of the coil decreases relative to its value if it were suspended in air as given below:

$$\boldsymbol{L = \frac{\forall}{I}} \qquad (1)$$

The presence of eddy currents in the test specimen also results in a resistive power loss. The effect of this power loss is manifested in the form of a small increase in the effective resistance of the coil. An exaggerated view of the changes in the terminal characteristics of the coil is

shown in Figure 1-2, where the variation in resistance and inductance is plotted in the impedance plane. When a flaw or in-homogeneity whose conductivity differs from that of the host specimen is present, the current distribution is altered. Consequently, the impedance of the coil changes relative to its value obtained with an unflawed specimen, as shown in Figure 1-2.

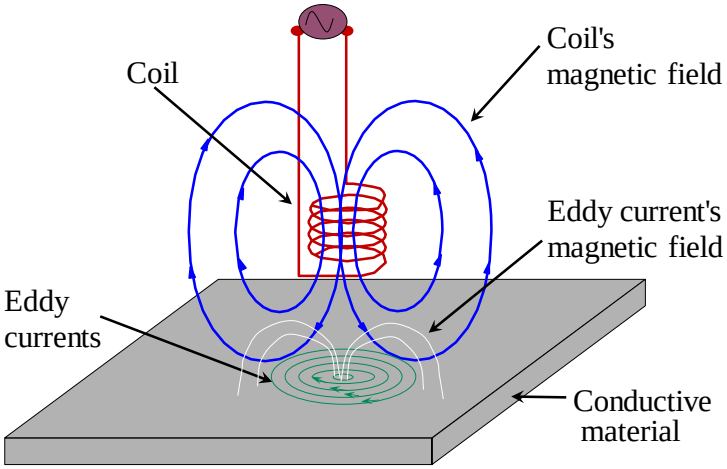

Figure 1-1 Principle of Eddy Current generation in specimen

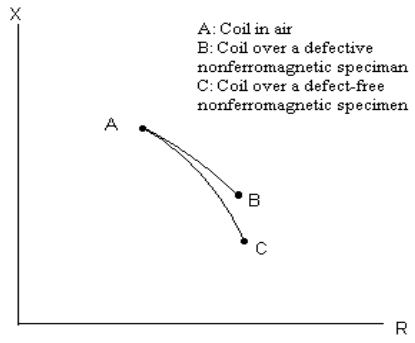

Figure 1-2 Formation of Eddy Current Signal on Impedance Plane

1.3.1 Multifrequency Eddy Current Testing

ET data acquired at different frequencies contain complementary information. ET data a low frequencies have longer penetration depths whereas ET data acquired at high frequencies offers better scan resolution. The set of frequencies would be determined based on skin depth calculation and nature of probable flaw. They can also be used to detect thickness loss due to of corrosion.

1.4 Research Objective

ET signal processing algorithm development for flaw diagnosis and profiling is a need of the hour. Therefore the objective of this research is to develop PC based software comprising of flaw diagnostics algorithms for detection and profiling of damage. Actual ET data can be injected in the software. Flaw detection and profiling report would be the output of the software. We have reports of air crashes every now and then; hopefully, this research will help to reduce such instances.

1.5 Organization of Dissertation

This thesis organizes as follows:

Chapter 2: Presents the brief introduction of data acquisition and interfacing of Eddy Current equipment with PC used in Pakistan International Airline for Non Destructing Testing. This section contains the description of data format analysis of raw data and standards used for calibration procedure.

Chapter 3: Present the proposed approach for flaw detection. The necessary equation along with the complete description of algorithms is presented. Results of applying these algorithms are also presented in the corresponding sections

Chapter 4: Present the proposed approaches to solving inverse problems namely, calibration curve and neural network algorithm respectively.

Chapter 5: Contains introduction of data fusion and the formulation of spatial frequency correlation method for solving corrosion quantification.

Chapter 6: Summarizes the thesis and presents ideas for future work

Figure 1-3 shows the complete multifrequency eddy current signal processing scheme.

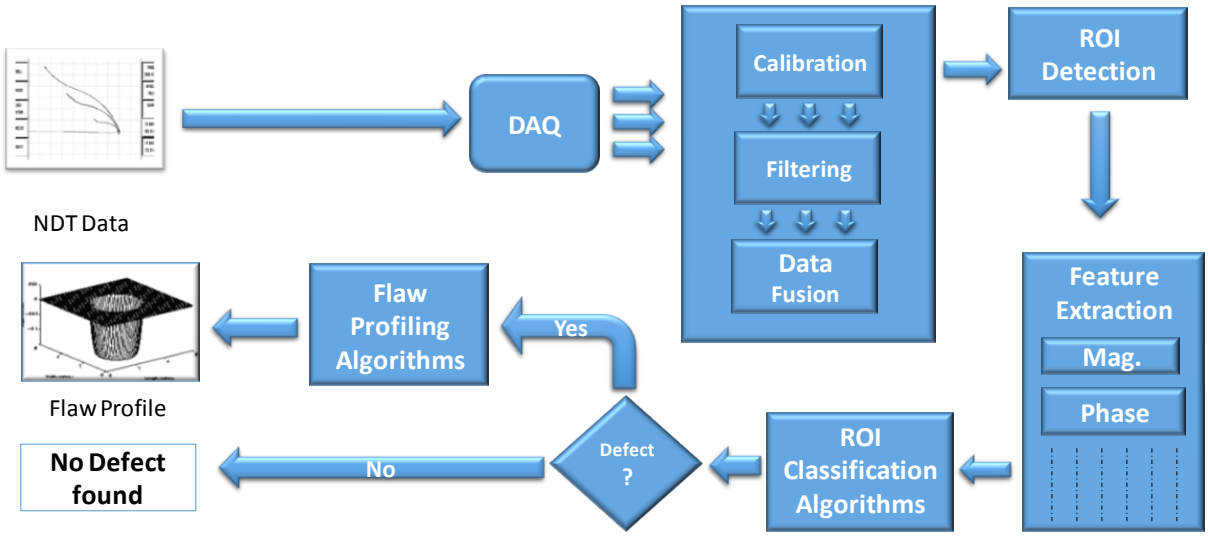

Figure 1-3 Eddy current signal processing scheme

CHAPTER 2

2 DATA ACQUISITION

The first and foremost task in the flaw detection and profiling algorithms requires the interfacing of the equipment with a computer. The current scope of project involves the application of Eddy Current techniques, therefore the equipments dealing with these techniques is required to be interface with the computer for further processing. The subsequent sections describe the procedures for interfacing the eddy current with computer.

2.1 Eddy Current Equipment

Multiple NDT Eddy current testing equipments are manufactured by multiple vendors, the available ones in PIA NDT lab is listed as under and shown in Figure 2-1

- NORTEC 2000S
- NORTEC 2000D

Since both the equipments have been manufactured by the same vendor, similar procedures are required for interfacing these equipments.

Figure 2-1 NORTEC 2000S Display

Prior to interfacing, eddy current NDT scan data needs to be stored in the equipment. NORTEC 2000S can store up to 20 programs with maximum 60 seconds reading. An RS232 serial interface is provided over NORTEC 2000S as shown in Figure 2-2 with 9600bps as its default baud rate. DB9 F/F straight through cable is used for connecting the equipment with the computer.

Figure 2-2 NORTEC 2000S I/O Ports

PIA does not have interface cables so necessary cables were procured along with the SERIAL to USB Converter, as the DB9 serial port is obsolete. Eddy Master software is the vendor provided software for extracting data**.** The software is design to assist PC based data acquisition from NORTEC 2000S equipment and it doesn't provide support for newer operating systems (Windows Vista and advanced). The data acquired through is shown in Figure 2-3

After completing the prerequisites along with connecting RS232 cable and making UART configurations, Eddy Master shows a pop up window that equipment has been connected. The default storage format is the .dat format in which Eddy current scan data gets stored. The next step is to analyze ".dat" format and calibration of instrument.

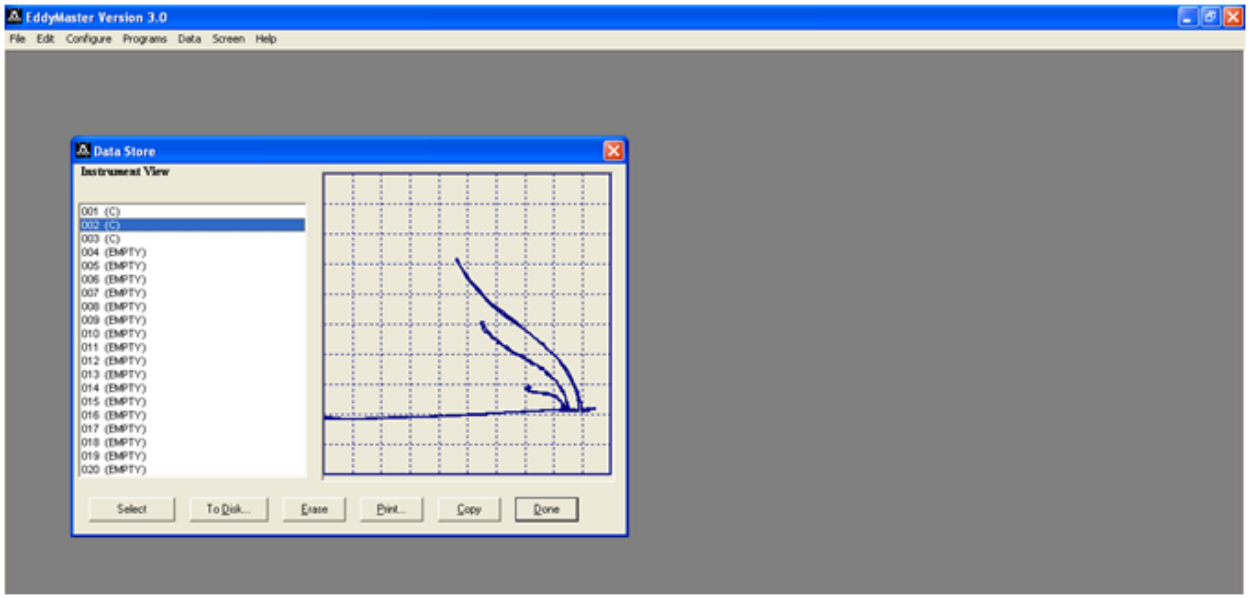

Figure 2-3 NORTEC 2000S Interface with PC

2.2 Data Format Analysis

The data retrieved from NORTEC 2000S has .dat file extension. DAT file extension is an abbreviation for DATA file and generally consists of text or numeric data. There are multiple

text processing tools that can be used for processing the .dat files. MATLAB as shown in Figure 2-4 has been the primary choice as it provides a large degree of freedom to the algorithm designers.

The general attributes of the .dat file that have been acquired from the NORTEC 2000S Eddy Current Equipment is listed as under.

- Header : 17 lines
- Data : 8324 lines

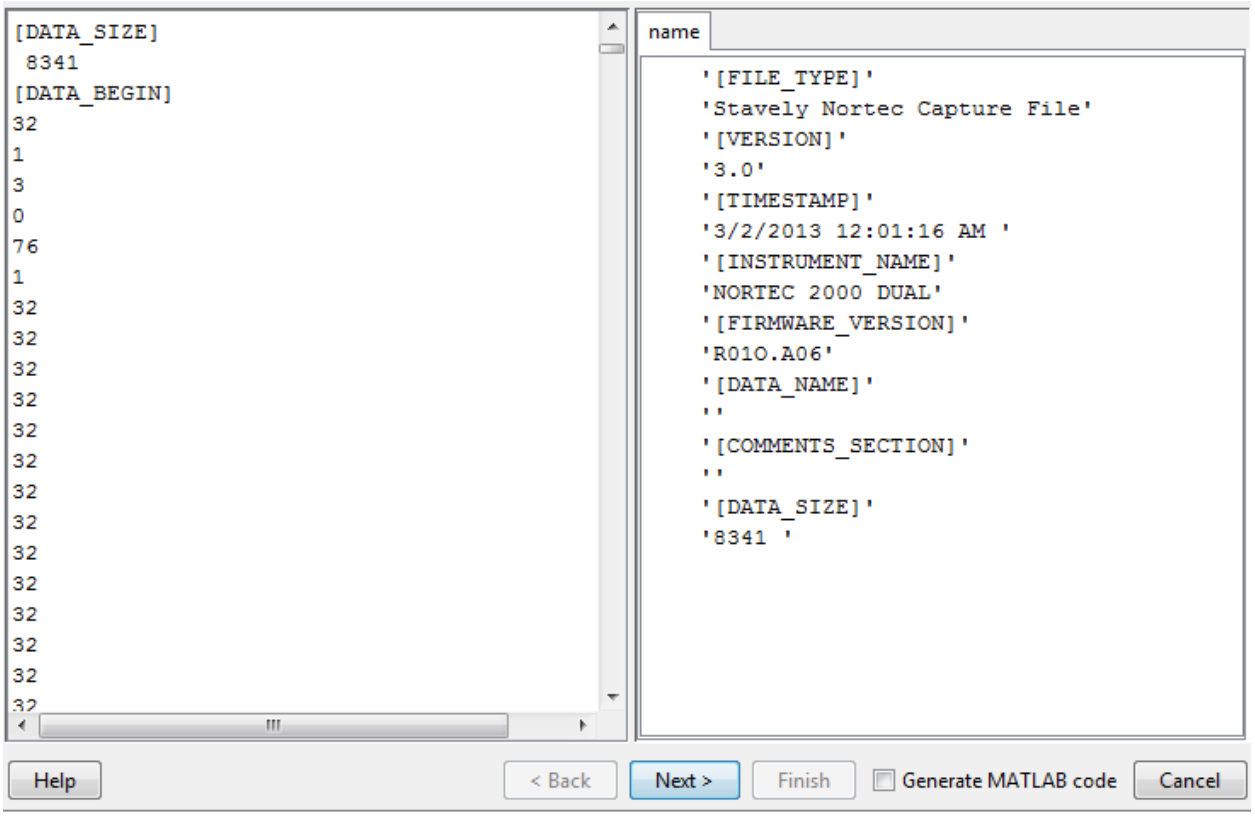

Figure 2-4 Data format Analysis in MATLAB

The first step involves the filtering of header from the .dat files as the header won't contribute any significant information about the structural defects. After performing iterative processing

over the acquired data, it was found that the first 363 lines and last 321 lines of data don't contribute any useful information; therefore the data is filtered out.

For data plotting in x-y plane, single column data was converted into double column format using alternate numeric values.

2.3 Calibration Procedure

The calibration of NORTEC 2000S and NORTEC 2000D equipment is carried out using GE Inspection Technologies Standard Calibration block having serial number of "S/N 320004/07 ". This block contains three notches of 0.2mm, 0.5mm and 1mm depth as shown in Figure 2-5 . The block is used in calibration of surface crack detection.

Figure 2-5 Calibration Block

Whenever NORTEC 2000S restarts it sets parameters with default value. To take measurement on reference standard, some important parameters need to be changed as follows:

- Frequency = 500 kHz
- Angle = 26^{o}
- Horizontal Gain = 68.0 dB
- Vertical Gain = 77.0 dB

After setting these values, sliding of probe over three notches give the results that matches with the results provided by the equipment manual and as shown in Figure 2-6.

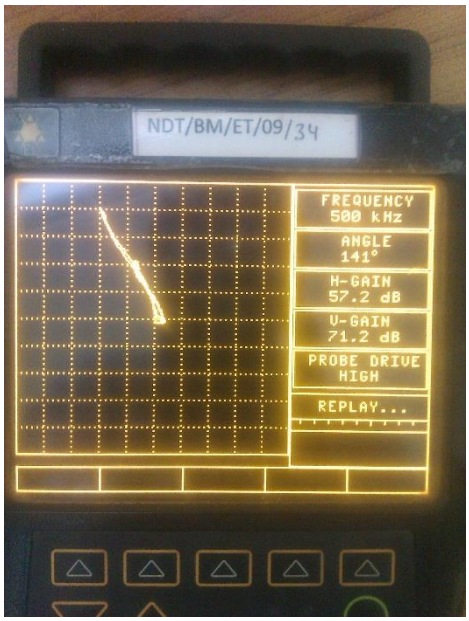

Figure 2-6 Display of Nortec 2000S from Calibration Block

2.4 Choice of Calibration Standard

Calibration standards are the reference blocks used extensively in the field of Non-destructive testing. These standards are provided by the aircraft manufacturer to the relevant Non-destructive testing section of the airline if they are performing NDT. These blocks are available for different parts of the aircraft, reference blocks are made of the same material as that of the aircraft components. These blocks are often embedded with artificial or self created well dimensional

cracks/flaws in order to estimate and detect the crack properly. Reference blocks are of different shapes and sizes developed by the manufacture as shown in Figure 2-7, there is a serial number mentioned against each block which helps in working with that block. This serial number is very helpful for record keeping of NDT. OEM provides the Non-destructive testing manual to inspect the concerned part, this manual comprises of the procedure and steps that NDT Team needs to perform for evaluation of the crack. In aircraft industry NDT manual is called an NTM used for Non-destructive inspection.

Figure 2-7 Reference Standards for B737 and A310 aircrafts

Choice of calibration standard is very important as different parameters have to be taken into consideration before performing NDT of the affected/diagnosed area. Few of them are mentioned below:

1. Choice of calibration standard depends on the component or a part being inspected, a block of the same area/components has to be selected as the area which is being inspected e.g. Fuselage, landing gear and wings in case of this project

2. Techniques that can be used on a calibration block as in this case only the reference blocks on which eddy current testing techniques can be performed have to be considered
3. Checking for the equipment as if either it is available or not, in most cases for ultrasonic testing USN 60 is being used at PIA and for eddy current testing NORTEC 2000S is being used, one of the reasons for the selection of this equipment for the project
4. In eddy current testing looking for probes/eddy current coil which can be used on calibration block for testing and data acquisition as shown in Figure 2-8
5. For ultrasonic testing on chosen calibration block one also needs to check for the available frequency transducers

Selection of calibration block needs proper reading of the material and manual as this selection will help in properly diagnosing the affected area. Calibration blocks for different aircraft are different i.e. one can't calibrate for Boeing 737 on the reference block given by manufacturer for same part of Air Bus 310.

Below tabulated are the few reference standards or calibration blocks details which have been finalized to be used in this project for eddy current testing:

Figure 2-8 Eddy Current Equipment Probes

Table 2-1 Reference Blocks for Eddy Current Testing

S.No	Part of the Aircraft	EDDY CURRENT TESTING	
		Boeing 737	Reference Block Serial No.
1	Fuselage	horizontal flange, strap, doubler and skin	A352
2	Landing Gear	upper and lower drag strut fuse bolt	380-X
3	Wings	wing center section rear spar lower chord	MP-905-50B

CHAPTER 3

3 FLAW DETECTION

3.1 Signal Preprocessing

For the implementation of effective algorithm schemes for flaw classification, efficient data processing procedures have to be applied. The designed data processing procedures are implemented as shown in Figure 3-1.

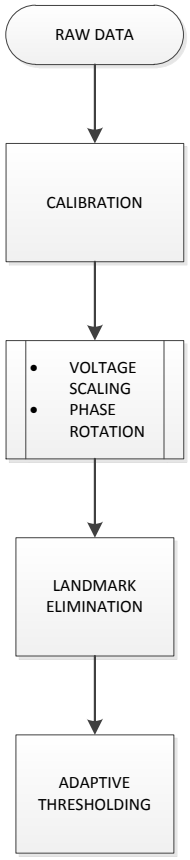

Figure 3-1 Signal Preprocessing Scheme

3.1.1 Calibration of Data

For accurate flaw detection, a standard has been taken of the same material as the aircraft part under inspection; this piece is then used to calibrate the instrument. The calibration of NORTEC 2000S equipment is carried out using GE Inspection Technologies Standard Calibration block having serial number of "S/N 320004/07 ". This block contains three notches at depths of 0.2mm, 0.5mm and 1mm as shown in Figure 2-5. The block is used in calibration of the instrument for surface crack detection. The raw data plot of "S/N 320004/07" acquired through NORTEC 2000S is shown in Figure 3-2.

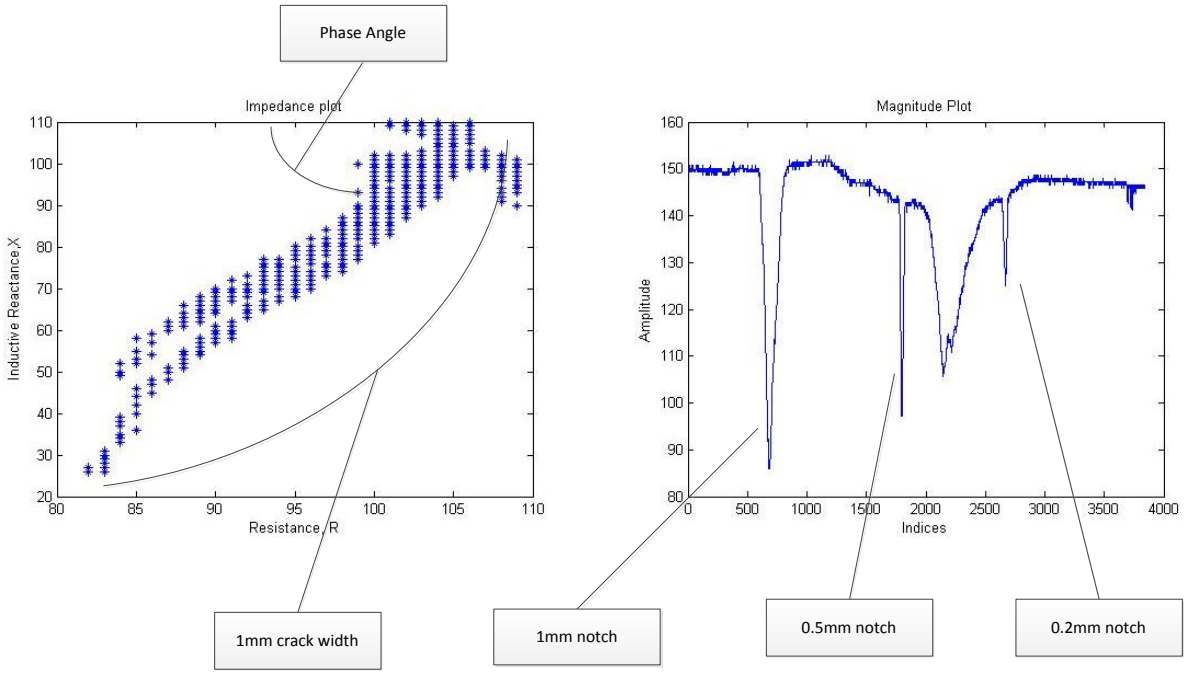

Figure 3-2 Impedance and Magnitude Plot of Eddy Current Data from Calibration Standard

Due to variation in the depth of cracks, the phase angle for each notch is different. However, in the magnitude plot, three peaks representing magnitude of different cracks can be observed.

The calibration procedure consists of two steps: voltage scaling and phase rotation.

3.1.1.1 Voltage Scaling

In voltage scaling, the magnitude of the signal corresponding to a deepest notch is first scaled to a fixed value. The raw data is then scaled by this same factor. The scaling factors are obtained by normalizing the maximum magnitude of the data from a 100% defect to a fixed value (usually 10 volts). The impedance in a circuit with resistance and inductive reactance can be calculated using the following equation.

$$\boldsymbol{Z = \sqrt{(R^2 + X^2)}} \qquad (2)$$

Where:

$Z =$ Impedence

$R =$ Resistance

$X =$ Inductive reactance

3.1.1.2 Phase Rotation

Eddy current testing (ECT) relies strongly on the relationship between flaw depth and signal phase. Phase analysis permits the differentiation of flaw signals from signals obtained from other sources such as deposits and support plates. A small surface defect and large internal defect can have a similar effect on the magnitude of impedance in a test coil. However, as the phase lag increases with depth, there will be a characteristic difference in the test coil impedance vector.

The illustration in Figure 3-2 presents the impedance plane representation of a signal from notches at three different depths. The signal is calibrated in instrument beforehand but when the data is transferred to the PC, the signal is formed with a rotated phase.

In eddy current data representation, the standard procedure is to calibrate the maximum eddy current signal at a phase of 35 degrees. The phase rotation step first identifies the phase angle of a 100% notch in the calibration standard. This can be done the by finding the indices of a matrix where maximum signal value occurs. The phase at that index is calculated by using the following equation:

$$\boldsymbol{\theta = tan^{-1}\frac{X}{R}} \quad (3)$$

Where:

$\theta =$ Phase angle

X = Inductive reactance

$R =$ Resistance

The difference between the phase angle corresponding to the 100% notch and the reference angle of 35^0 is then calculated, which gives the angle of rotation that needs to be applied to rotate the signal. This process is carried out for each channel of data by multiplying the raw data with the rotation matrix. The rotation matrix can be calculated by using the following formula:

$$\boldsymbol{R = \begin{bmatrix} cos\,\theta & sin\,\theta \\ -sin\,\theta & cos\,\theta \end{bmatrix}} \quad (4)$$

Where:

$R =$ Rotation matrix

θ = Difference between reference angle and phase angle of raw data

The data is then subtracted from the maximum value of x and minimum value y in order to center it at the origin. Figure 3 shown below illustrates the scaled and rotated signal after calibration.

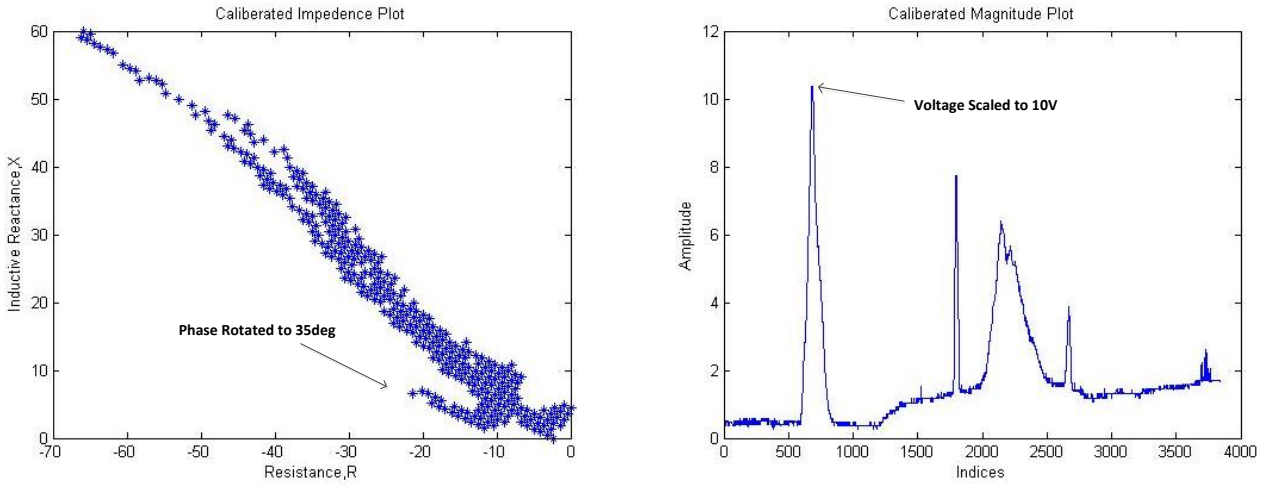

Figure 3-3 Calibrated Impedance and Magnitude Plot

3.1.2 Land Mark Elimination

The aircraft structures are riveted on one another. When eddy current testing is carried out, these rivets are also detected as cracks. These are basically the land marks because they occur at fixed positions. To demonstrate how to eliminate land marks from the data, a Fokker Aircraft plate with holes was inspected. The plate was divided into 9 rows and 11 columns as shown in Figure 3-4, with each grid having 10mm side length and two cracks of different sizes at different locations.

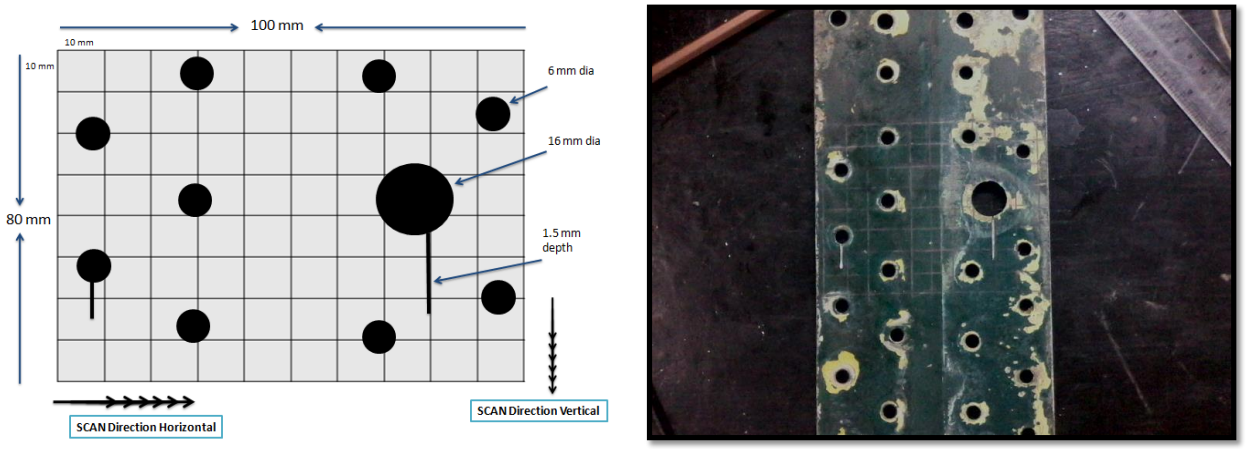

Figure 3-4 Fokker Aircraft Plate for Eddy Current Inspection

Eddy current testing of Fokker Aircraft plate was performed. The raw data plot of inspection plate is shown in Figure 3-5.

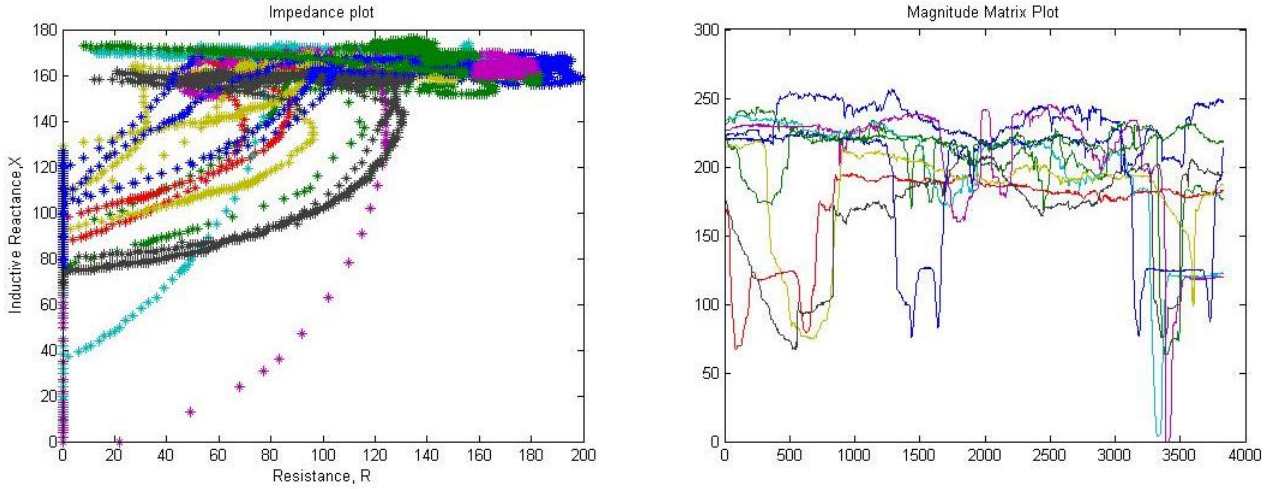

Figure 3-5 Impedance Plot and Magnitude Plot of Eddy Current Data from Fokker Plate

As it can be seen through Figure 3-5, there is a great amount of noise present in the signal due probe lift off, unevenly coated surface, high frequency noise and land marks in the plate. The first step in data processing is to calibrate the raw data from the values calculated through

Equation (3) and (5). Image processing techniques were then applied on calibrated raw data to eliminate noise and land marks.

Image processing techniques are valuable for the accurate and consistent interpretation of signals in non destructive testing. It performs important functions in data analysis, ranging from simple noise filtering for enhancing the signal to noise ratio to automated signal classification.

The image plot of data acquired from the inspection plate after its calibration is shown in Figure 3-6.

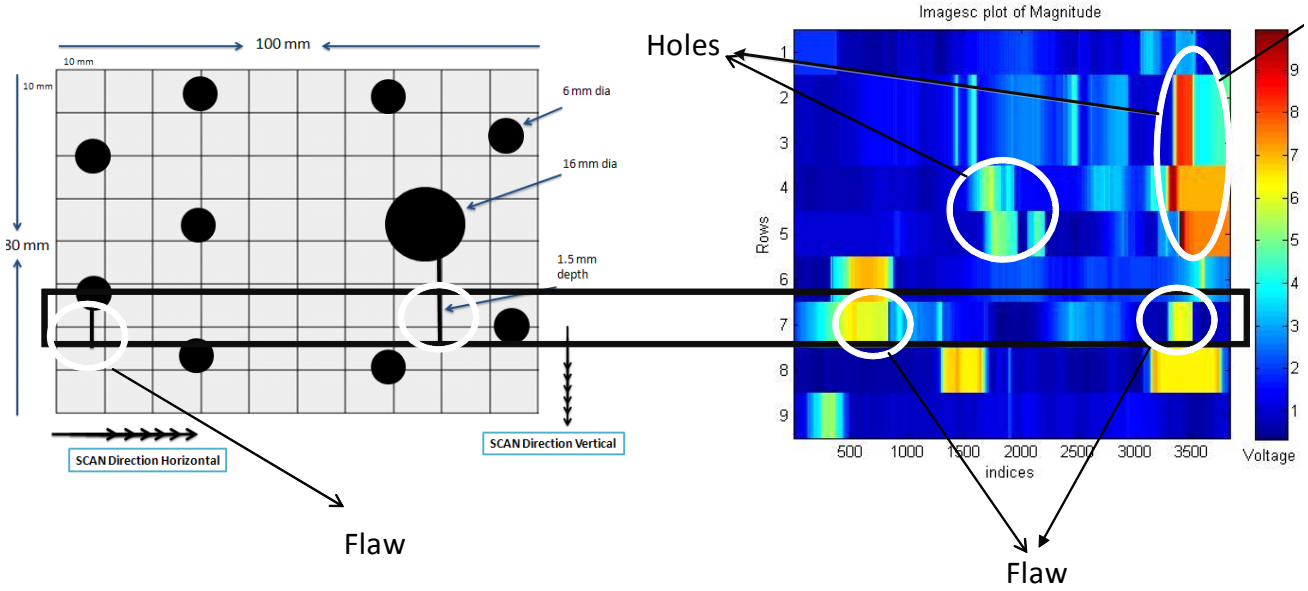

Figure 3-6 Calibrated Image of Fokker Plate Raw Data

The image function scales image data to the full range of the RGB color map and displays the image. The image formed in Figure 3-6 varies in colors with respect to cracks, holes and non-defect areas. For land mark elimination, the areas where higher values of color exist are replaced by non defect area values, as we get the maximum signal from the areas where the holes exist. The image formed after the land mark elimination process in shown in Figure 3-7.

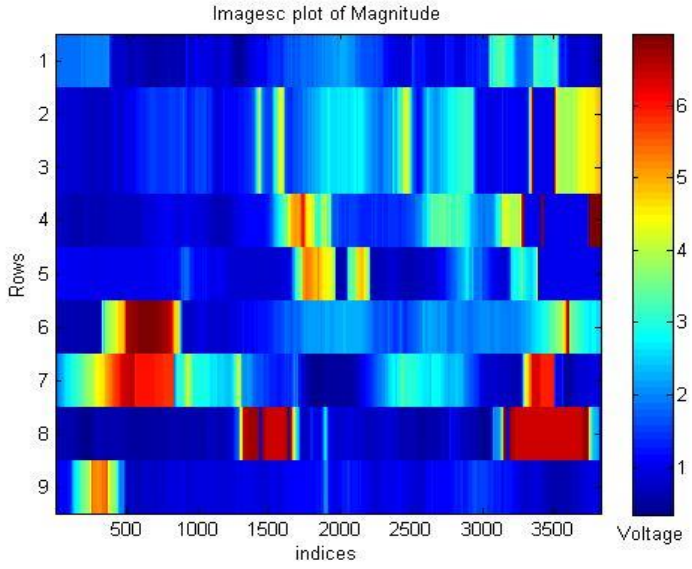

Figure 3-7 Image of NDT data from Fokker Plate after Land Mark Elimination

3.1.3 Adaptive Thresholding

In order to extract valuable information from the image shown in Figure 3-7, we first need to divide the image into distinctive components, which can then be further analyzed and cracks can be separated from landmarks.

Thresholding is used to segment an image by setting all pixels whose intensity values are above a threshold to a foreground value and all the remaining pixels to a background value. In order to overcome the ill influence of noise, it becomes necessary to take it into consideration when selecting the threshold being used. On the other hand, this is an impossible mission in a global context, since no one threshold can fit the entire image. This leads to the conclusion, that a more local threshold must be used. The locality property can allow a few cautious assumptions, and according to these assumptions, produce a suitable threshold for the pixels in the environment.

Adaptive thresholding is used to remove this ill influence which typically takes a grayscale or color image as input and, in the simplest implementation, outputs a binary image representing the segmentation. For each pixel in the image, a threshold has to be calculated.

Eddy current data collected from different locations in the inspection plate possess different signal characteristics and hence different thresholding schemes are utilized based on the quality of data in hand. The first thresholding scheme is very simple and it includes two procedures: one for magnitude and the other for phase. In magnitude thresholding, signals whose magnitude is less than the threshold level are treated as noise and set to zero. In phase thresholding or 'phase gating', signals with phase angles below the flaw plane are eliminated with only those signals whose phase angle lies in the flaw plane being retained.

Magnitude thresholding as proposed here is based on the use of an adaptive thresholding scheme that optimally varies the threshold value for different regions in the plate. This scheme computes the histogram of voltage values as shown in Figure 3-8 by assigning voltages at each pixel location to one of several bins. The threshold is then computed as:

$$t = \mu + K\left[\max\left(V_L\right) - \min\left(V_L\right)\right] \quad (5)$$

Where:

μ = Median of the voltage values in a local (segmented) region of the image

V_L = Set of voltage values that lie in three bins around the median value in the voltage histogram of the local (segmented) region of the image

K = Constant, chosen based on the magnitude of the 20% defect in the corresponding calibration block.

t = Threshold chosen for the local region

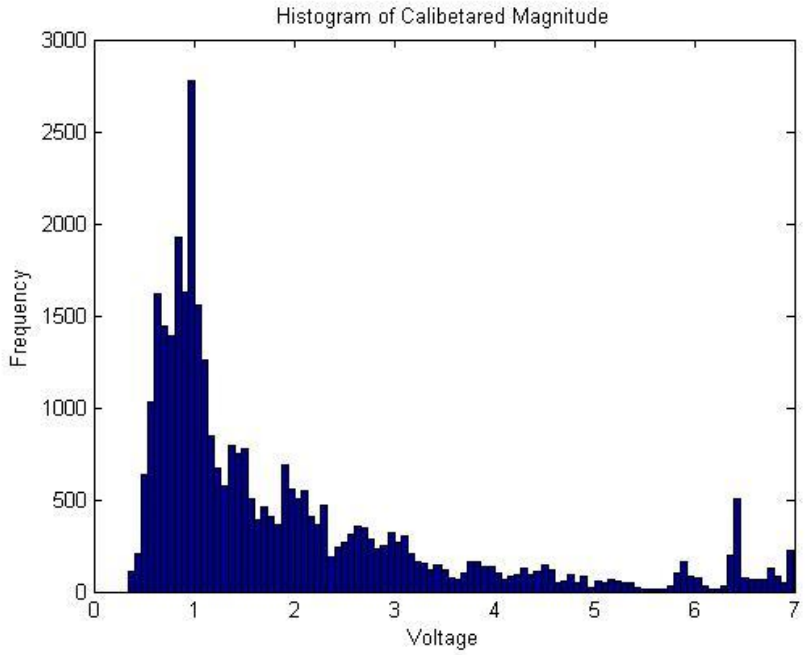

Figure 3-8 Histogram of Eddy Current Measurements

A single threshold computed using mean μ and standard deviation σ of the data collected from more than one region often yields sub-optimal performance during flaw detection. A variation of the adaptive thresholding algorithm that computes individual thresholds for data from different plate sections based on their local statistics may be used in such cases. This variation in the flaw detection scheme can be represented mathematically as follows and the result is shown in Figure 3-9.

$$x_k = \begin{cases} flaw, & |x_k| \geq \tau_r \\ noise, & |x_k| < \tau_r \end{cases} \quad (6)$$

Where:

$\tau_r = \eta.percentile\ \left(X^r\right)$ is threshold for sample x_k .

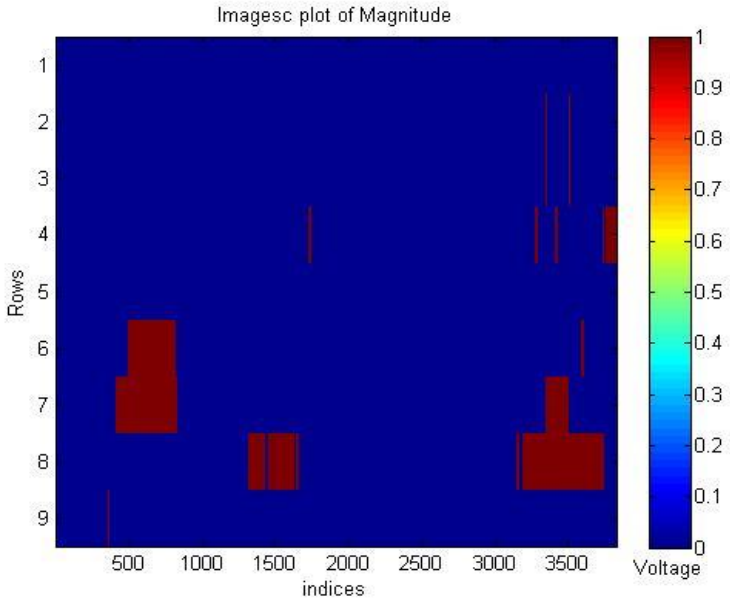

Figure 3-9 Image formed after Adaptive Thresholding Algorithm

3.2 Region of Interest (ROI) Detection

The image formed after applying adaptive thresholding scheme is in binary format. Binary images may contain numerous imperfections. In particular, the binary regions produced by thresholding are distorted by noise and texture. To find potential region of interest in Figure 3-9, a morphological operation has to be performed. Morphological image processing pursues the goals of removing these imperfections by accounting for the form and structure of the image.

Morphological image processing is a collection of non-linear operations related to the shape or morphology of features in an image. Morphological operations rely only on the relative ordering of pixel values, not on their numerical values, and therefore are especially suited to the processing of binary images. Morphological techniques probe an image with a small shape or template called a structuring element. The structuring element is positioned at all possible locations in the image and it is compared with the corresponding neighbourhood of pixels. Some

operations test whether the element ‘fits’ within the neighbourhood, while others test whether it ‘hits’ or intersects the neighbourhood. When a structuring element is placed in a binary image, each of its pixels is associated with the corresponding pixel of the neighbourhood under the structuring element. The structuring element is said to fit the image if, for each of its pixels set to 1, the corresponding image pixel is also 1. Similarly, a structuring element is said to hit, or intersect, an image if, at least for one of its pixels set to 1 the corresponding image pixel is also 1.

The ROI detection in Figure 3-10 is done by using two different functions of MATLAB namely: ‘majority’ and ‘clean’.

‘Majority’ function sets a pixel to 1 if five or more pixels in its 3-by-3 neighborhood are 1s; otherwise, it sets the pixel to 0, however ‘clean’ function removes the isolated pixels (individual 1s that are surrounded by 0s) from the image.

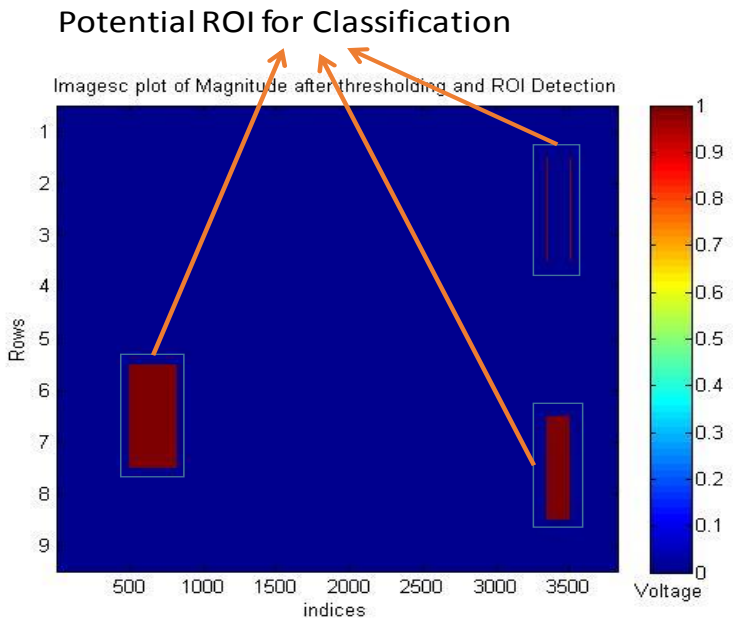

Figure 3-10 Potential ROI detection using Morphological operation

3.3 Feature Extraction

In feature extraction, characteristic features that contain discriminatory information are extracted and identified. These features serve as the compact signature of the signal. Features are the data attributes that capture the similarities in signals of the same class and dissimilarities in the signal from a different class. It can be physical or transform based.

Once the preprocessing algorithms identify regions of interest (ROI) in each data file, a classification algorithm is applied to classify each ROI into one of several classes on the basis of its features. So for this purpose, numerous features of each ROI have been identified such as phase, magnitude, flaw length, phase trends and continuous wavelet transform coefficients.

Figure 3-10 shows the thresholded image of the Fokker Aircraft plate in which three indications have been identified. Features are extracted for each of these regions of interest and processed individually by the classification routines. The objective is to distinguish flawed from non-flawed areas.

3.4 Classification

Once the features are computed, the classification step is use to eliminate redundancy and evaluate the features on the basis of the discriminatory information. Therefore, a decision tree algorithm is employed to identify key features that contain the most amount of discriminatory information. These features then form the input to a rule base to classify the indication as a defect or a non-defect. Figure 3-11 shows the feature extraction and classification scheme.

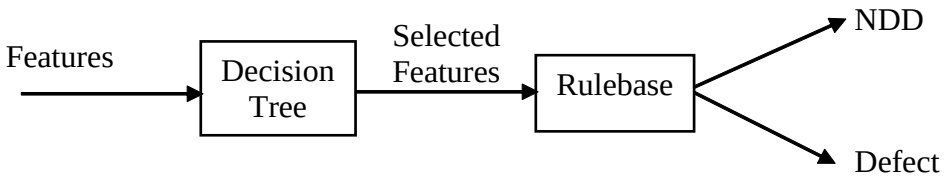

Figure 3-11 Feature Extraction and Rule Base Classification Process

The rule base is a set of heuristically obtained rules that are applied sequentially to eliminate false calls, and retain true defect indications. Most of the rules are based on the features that are available at the output of the decision tree stage. In addition, a small set of other features are also chosen heuristically (based on expert knowledge) to form additional rules. The rules are then constructed by a choosing a weighted combination of these features and a threshold, so that optimal classification performance is achieved. A Boolean expression is also used in many cases to combine different rules.

3.5 Results

After the classification of ROI's into defect and non defect regions, the report has been generated which gives adequate detail about the effected regions. The report generated after the inspection of Fokker Plate which contains 4 defected regions is shown in Table 3-1.

Table 3-1 Report Generated after Inspection of Fokker Plate

::Eddy Current Test Report::

Engineer: Moez-ul-Hassan
Date: 15-Jan-2014

Number of ROIs: 4

ROI#	ROI Locations	Features	Value	Decision
1	2	MaxVert	6.128101	NO DEFECT
	3	MaxMag	6.893474	
	3345	Phs_200	62.000000	
	3358	Phs_100	85.000000	
2	2	MaxVert	6.068026	DEFECT
	3	MaxMag	6.518175	
	3505	Phs_200	68.000000	
	3509	Phs_100	58.000000	
3	6	MaxVert	6.113297	DEFECT
	7	MaxMag	6.998530	
	494	Phs_200	60.000000	
	824	Phs_100	61.000000	
4	6	MaxVert	6.223149	DEFECT
	8	MaxMag	6.415339	
	3343	Phs_200	75.000000	
	3498	Phs_100	43.000000	

::End of Report::

The second column in Table 3-1 represents the location of potential regions in terms of rows and columns. The features such as maximum reactance, maximum magnitude, phase at 200 kHz and phase at 100 kHz are extracted from defined location. The values of the extracted features are placed in third column of Table 3-1. Classification of the ROI is done using heuristically defined rule and result is shown in the last column i.e. either the detected ROI contains “DEFECT” or “NO DEFECT”.

CHAPTER 4

4 FLAW PROFILING

4.1 Defect Characterization

Once the flaw/damage is detected, the next step is to quantify the damage in order to understand the criticality of the damage. Flaw profiling from NDT data is a typical inverse problem. The inverse problem is ill-posed due to non-uniqueness, non existence and instability of the solution. In order to address the ill-posedness deterministic as well as statistical techniques could be used to solve the inverse problem.

Flaw Profiling/characterization refers to the estimation of depth profile of defects from the corresponding measurement signal as shown in Figure 4-1. Several factors contribute to distortion of the measured eddy current signal. One example is the limitation of the inspection system relative to resolution of the flaw segments that make up the entire flaw length. The different characterization algorithms implemented for defect profiling are explained in this section.

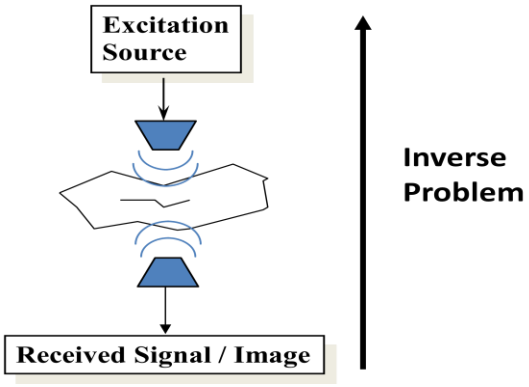

Figure 4-1 Estimation of Depth Profile from Measurement

4.2 Calibration Curves

One of the earliest and most widely used approaches is the calibration method. A calibration curve of defect depth versus magnitude and phase is constructed using known defects signals in a calibration standard of a particular aircraft part with machined defects of varying depths. Figure 4-2 shows typical calibration standard curves constructed for defect profiling. This method is currently used in industry to generate estimates of the one-dimensional profile of a defect.

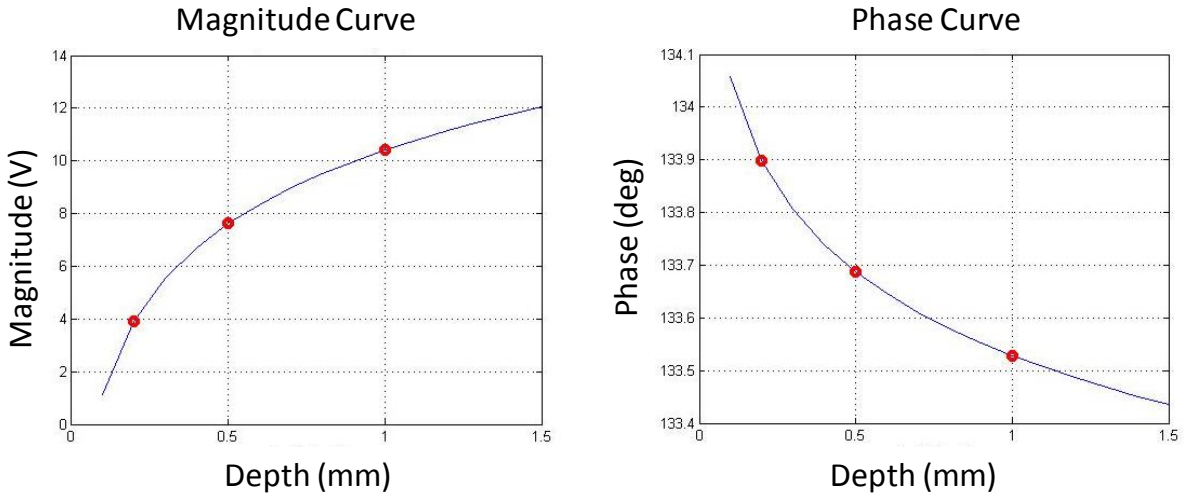

Figure 4-2 Calibration standard Curves of Magnitude and Phase

For a given defect signal, the equivalent length, width and depth of the defect are predicted using the calibration curve along with 'logfit' interpolation function. 'Logfit' function applies the "least squares" method to fit the logarithmic equation to the data. The graph of the equation is a logarithmic curve moved horizontally by *c* and possibly mirrored across the y-axis. For instance, a calibration curve that relates the phase, amplitude or magnitude of the eddy current signal with the depth of the defect can be represented by a relationship of the form,

$$\boldsymbol{y = a + b * \ln(sign * (x - c)), sign = +1, -1} \quad (7)$$

The formula is then rearrange in terms of slope and intercept form to calculate the unknown. This is non-linear fitting by trial-and-error.

4.3 General Regression Neural Networks

An alternate approach is to use a learning algorithm that implements function approximation using general regression neural network (GRNN). Mathematically, this approach yields a highly nonlinear mapping from an input vector space on to an output vector space. GRNN is a variation of the radial basis neural networks. A GRNN does not require an iterative training procedure as back propagation networks. It approximates any arbitrary function between input and output vectors, drawing the function estimate directly from the training data. In addition, it is consistent that as the training set size becomes large, the estimation error approaches zero, with only mild restrictions on the function. GRNN have demonstrated their usefulness in both linear and non linear processes involving many variables and even in the presence of noisy data. A typical architecture of GRNN is shown in Figure 4-3.

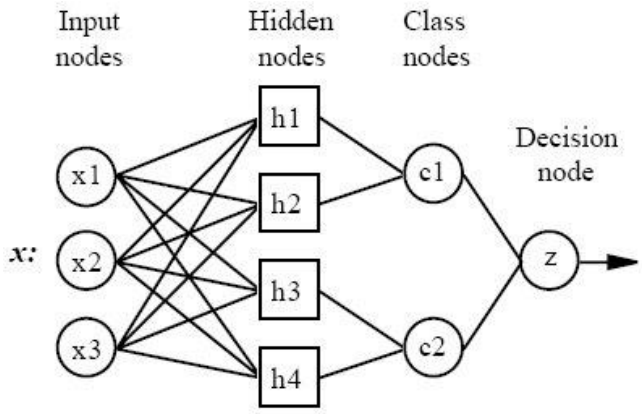

Figure 4-3 Architecture of GRNN

The input-output transformation equation for the GRNN can be expressed as

$$\boldsymbol{Y(X)} = \frac{\sum_{i=1}^{n} \boldsymbol{Y_i} \exp\left(-\boldsymbol{D_i^2}/\boldsymbol{2\sigma^2}\right)}{\sum_{i=1}^{n} \left(-\boldsymbol{D_i^2}/\boldsymbol{2\sigma^2}\right)} \quad (8)$$

$$\boldsymbol{D_i^2} = (\boldsymbol{X} - \boldsymbol{X_i})^{\boldsymbol{T}} . (\boldsymbol{X} - \boldsymbol{X_i}) \quad (9)$$

where X is the input vector of dimension N and Y is output vector of dimension M. The distance, Dj, is the Gaussian distance between the training sample and the point of prediction, and is used as a measure of how well the each training sample can represent the position of prediction, X. The spread σ_i are computed during the training process using a training data set. The larger spread is, the smoother the function approximation will be. To fit data closely, smaller spread has been used than the typical distance between input vectors.

The general regression neural network has been designed by using Matlab function 'newgrnn'. 'newgrnn' creates a two-layer network. The first layer has 'radbas' neurons, and calculates weighted inputs with 'dist' and net input with 'netprod'. The second layer has 'purelin' neurons, calculates weighted input with 'normprod', and net inputs with 'netsum'. Only the first layer has biases.

4.4 Results

For the training of neural network for depth prediction, the sequence of algorithms shown in Figure 4-4 has been employed.

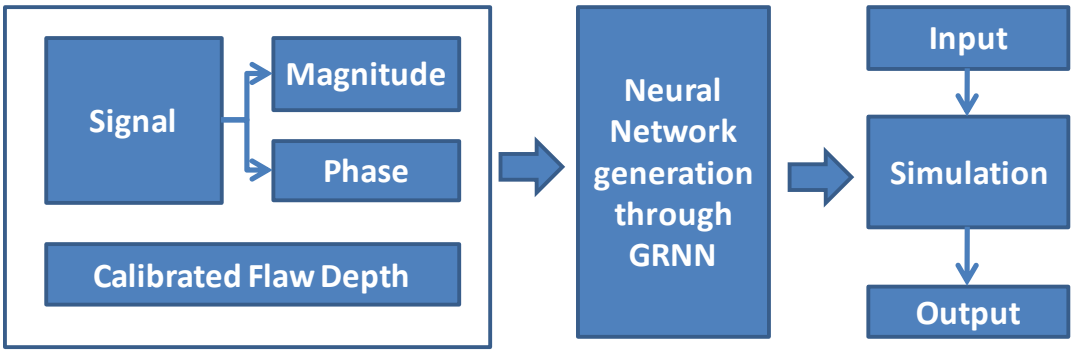

Figure 4-4 Schematic of the overall approach using GRNN

The data is collected from NDT Standard as shown in Figure 2-5 using three different frequencies i.e 200 KHz, 300 KHz and 500 KHz respectively. The network is trained by given the phase and magnitude values at particular standard depths i.e. 0.2mm, 0.5mm and 1mm respectively. We have 18 inputs which correspond to 3 targeted values which are actually the depths. The values of Input Matrix 'P' and Target Matrix 'T' for the training of GRNN are shown below in Table 4-1 along with the simulation result of estimated depth.

Table 4-1 Training Data and Flaw Estimation using sample data

Features	Frequency in KHz	Depth in mm		
		0.2	0.5	1
Magnitude	200	3	6.5	9.5
	300	3.5	7	10
	500	3.9	7.6	10.4
Phase	200	140.5	133.8	133.8
	300	140	133.8	133.6
	500	133.9	133.7	133.5

T= Target Matrix

P= Input Matrix

Input = [3 4 4.1 136 137 137]' → Output/ Estimated Depth = 0.3299mm

The neural network performance is significantly better than that obtained using conventional calibrated method largely due to the fact that is utilizes all information available from multiple frequency inspections.

CHAPTER 5

5 CORROSION QUANTIFICATION

5.1 Spatial Frequency Correlation based Data Fusion

Aging aircraft structures are prone to corrosion, which weaken the damage tolerance capability and accelerate the growth of cracks within the structures. To investigate structural integrity or to validate repairs, corrosion quantification techniques (or equivalently, thickness loss calculations) are considered important. Eddy current, useful NDT techniques capable of measuring corrosion in these structures

To deal with corrosion quantification, data fusion techniques have also been investigated. Many researchers have employed data fusion techniques to solve the NDE inverse problem. Commonly proposed solutions include neural networks, Bayesian analysis based on Dempster-Shafer evidence theory, wavelet and other multi-resolution algorithms and image fusion in time and frequency domain. These methods have been applied to fuse NDE data from a range of sources, including multi-frequency eddy current measurements and other measurement types such as pulsed eddy current measurements [16, 17].

Eddy Current data acquired at different excitation frequencies contains complementary information. Therefore, to obtain measures with sensitivity, a novel spatial frequency correlation based data fusion method has been developed for multi frequency eddy current measurements. In the proposed technique, the spatial information of multi frequency eddy current measurement coupled with frequency information to improve the characterization results. The technique presented in this paper is highly motivated by data fusion method based on spatial temporal correlation [18].

Spatial temporal correlation is a powerful technique as it produces different spatial temporal correlation fusion results in different applications. In recent years, spatial temporal correlation brings a significant application in the data fusion of most popular research directions i.e. wireless sensor network [19] and robust adaptive tracking [20]. Spatial Temporal based correlation also produced amazing results in multi neuron spike response [21] and imaging of brain activity in humans [22], as it directly fit to the physiological data.

The formulation of proposed spatial frequency correlation based data fusion method for multi frequency eddy current data fusion is given in Section 5.2. This is followed by an aerospace NDT case study, in which ET data of aircraft lap joint acquired at four different frequencies is fused using proposed formulation. The results are then presented in Section 5.3. Finally discussion on results along with concluding remarks is given.

5.2 Problem Formulation

In aerospace NDT, eddy current measurements from aerospace structures are acquired at multiple frequencies. In the proposed method, the data fusion of multi frequency eddy current signals has been performed by considering the correlation between space and frequency of the practical data. The complete architecture of proposed technique for image fusion is as shown in Figure 5-1. The algorithm starts executing with the initialization of data matrix containing spatial and frequency information of multi frequency eddy current data. The spatial frequency correlation of applied data is then calculated at each position index. In the next step, weight of each sample is computed through consistency and stability measurement of spatial frequency correlation matrix. For final data fusion and damage detection, multiplication of normalized weights with actual data has been performed.

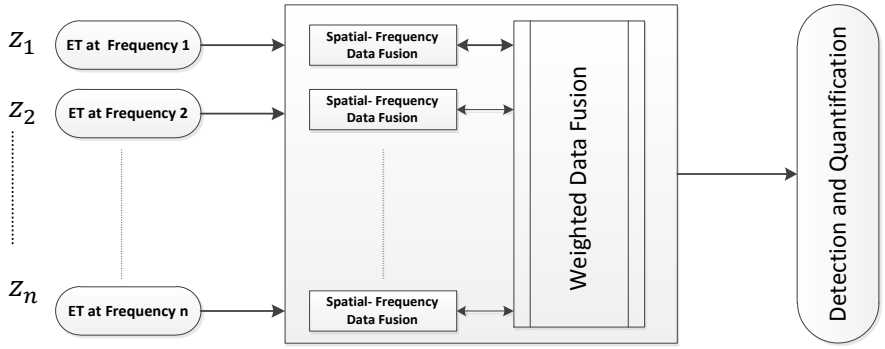

Figure 5-1 Architecture of Spatial Frequency Correlation based Data Fusion Technique

Considering $z_i(k)$ is the measurement of i^{th} frequency data, where i is the running indices, from eddy current probe at k^{th} time interval. So the output matrix of multi frequency measurement system within the time instantm is as below:

m = spatial data points

$$\boldsymbol{Z(m)} = \begin{bmatrix} \boldsymbol{z_1(1)} & \boldsymbol{z_1(2)} & \dots & \boldsymbol{z_1(m)} \\ \boldsymbol{z_2(1)} & \boldsymbol{z_2(2)} & \dots & \boldsymbol{z_2(m)} \\ \vdots & \vdots & \ddots & \vdots \\ \boldsymbol{z_n(1)} & \boldsymbol{z_n(2)} & \dots & \boldsymbol{z_n(m)} \end{bmatrix}_{\boldsymbol{n\times m}} \quad \text{n = number of frequency} \qquad \textbf{(10)}$$

From Equation (11), rows $[z_i(1) \quad z_i(2) \quad \dots \quad z_i(m)]$ in matrix $Z(m)$ contain the spatial information of eddy current data and columns$[z_1(k) \quad z_2(k) \quad \dots \quad z_n(k)]^T$ contain the frequency information of multi frequency eddy current measurement system. Since $z_i(m)$ and $z_j(m)$ represents the eddy current data at two different frequencies, therefore the spatial frequency correlation between $z_i(m)$ and $z_j(m)$ is as below:

$$\boldsymbol{\rho_{ij}} = \frac{\sum_{k=1}^{m} \boldsymbol{z_i(k) z_j(k)}}{\left(\sum_{k=1}^{m} \boldsymbol{z_i^2(k) z_j^2(k)}\right)^{1/2}} \qquad \textbf{(11)}$$

ρ_{ij} can be used to determine the spatial frequency correlation degree between $z_i(m)$and$z_j(m)$. The value of $0 \leq \rho_{ij} \leq 1$depends upon how different frequencies measurement are correlated with each other. The value of $\rho_{ij} = 1$ when measurements are exactly the same. According to Equation (12) the spatial frequency correlation matrix for n number for frequencies within time instant$m$ is stated as below:

$$\boldsymbol{R} = \begin{bmatrix} \boldsymbol{\rho_{11}} & \boldsymbol{\rho_{12}} & \cdots & \boldsymbol{\rho_{1n}} \\ \boldsymbol{\rho_{21}} & \boldsymbol{\rho_{22}} & \cdots & \boldsymbol{\rho_{2n}} \\ \vdots & \vdots & \ddots & \vdots \\ \boldsymbol{\rho_{n1}} & \boldsymbol{\rho_{n2}} & \cdots & \boldsymbol{\rho_{nn}} \end{bmatrix}_{\boldsymbol{n \times n}} \quad \textbf{(12)}$$

The horizontal vector $[\rho_{i1} \quad \rho_{i2} \quad \cdots \quad \rho_{in}]$ in Equation (13) describes the correlation between the i^{th} frequency and other frequencies signal. Through matrix R the consistency $q_i(m)$ can be measured as below:

$$\boldsymbol{q_i(m) = \frac{1}{n}\sum_{j=1}^{n} \rho_{ij}} \quad \textbf{(13)}$$

The final real time weight $p_i(m)$ of the i^{th} frequency data at m time instant is the function of consistency measurement $q_i(m)$ and stability measurement $\sigma_i(m)$ of multi frequency measurement system as described below:

$$\boldsymbol{P(m) = f\big(Q(m), \sigma(m)\big)} \quad \textbf{(14)}$$

The calculation of stability vector $\sigma_i(m)$ within the time instant$m$ to induce $p_i(m)$ is as follows:

$$\boldsymbol{\sigma_i(m) = \left[\frac{1}{m}\sum_{k=1}^{m}\left(z_i(k) - \frac{1}{m}\sum_{l=1}^{m} z_i(l)\right)^2\right]^{1/2}} \quad (15)$$

Considering the consistency measurement $Q(m) = [q_1(m) \quad q_2(m) \quad ... \quad q_n(m)]$ and stability measurement $\sigma(m) = [\sigma_1(m) \quad \sigma_2(m) \quad ... \quad \sigma_n(m)]$ of multi frequency measurement system, the exponential model of $p_i(m)$ is defined as below:

$$\boldsymbol{p_i(m) = q_i(m)e^{1-a\sigma_i(m)}} \quad (16)$$

Variable a is the coefficient$(0 < a \leq 1)$. For the final data fusion result, weight vector $p_i(m)$ from equation (7) must satisfy the condition of $\sum_{i=1}^{n} p_i(m) = 1$. The normalized weights from $p_i(m)$ are used to calculate the data fusion result. The data fusion result $F_r(m)$ at m time instant is the function of normalized weight from $p_i(m)$ i.e. p_i^{norm} and actual data $z_i(m)$. Therefore, at m^{th} time instant, the spatial frequency data fusion result of multi frequency measurement system is:

$$\boldsymbol{F_r(m) = \sum_{i=1}^{n} z_i(m)p_i^{norm}(m)} \quad (17)$$

5.3 Results

There are several research and development technologies being explored in the field of corrosion quantification, special thrust of the research is focused on detecting hidden corrosion in aircrafts.

For the application of spatial frequency correlation based data fusion method, a case study has been performed in which the eddy current measurement data was taken from 30-year old service-retired Boeing 727 aircraft aluminum lap joint cut [23] as shown in Figure 5-2.

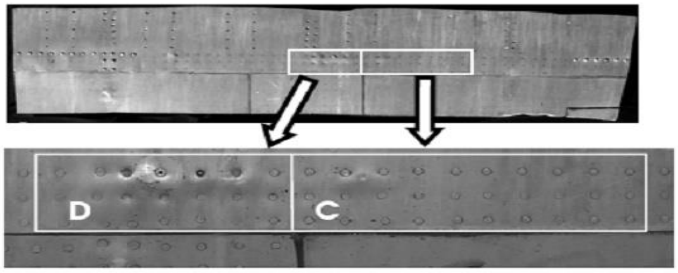

Figure 5-2 Aircraft Lap Joint Cut

The data was acquired at 30Khz, 17Khz, 8Khz and 5.5Khz frequencies as shown in Figure 5-3.

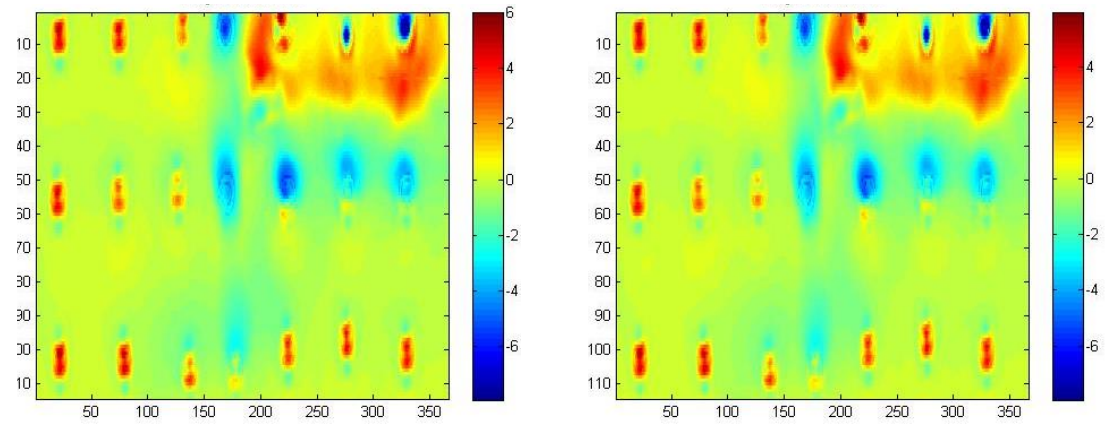

(a) ET at 30KHz

(b) ET at 17KHz

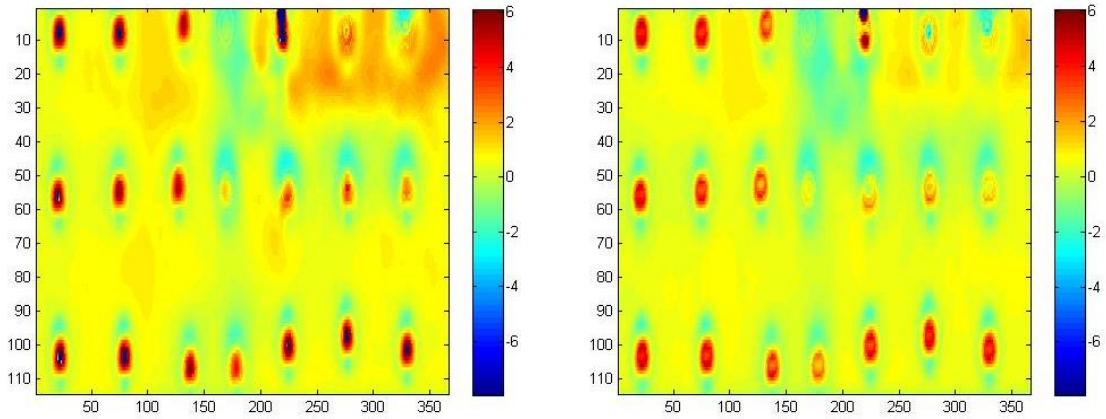

(c) ET at 8KHz

(d) ET at 5.5KHz

Figure 5-3 Eddy Current Measurements (Impedance Magnitude) of Specimen

In order to convert color image into binary format a threshold has to be calculated. However, it is impossible to fit the entire image with the single threshold due to of large histogram modes. Therefore to overcome this ill influence of noise and shading in the image Adaptive Thresholding has been applied to the eddy current measurement for improved results. In corrosion detection Adaptive Thresholding often yields sub-optimal performance. A single threshold has been computed using mean and standard deviation of the data collected from more than one region of eddy current measurement. 92% elimination has been applied on histogram, to attain the final binary image. The binary image formed after applying histogram based adaptive

thresholding scheme on aircraft specimen is shown in Figure 5-4, which may contain potential regions of interest. The rivets are removed from the adaptive thresholded image during the preprocessing scheme.

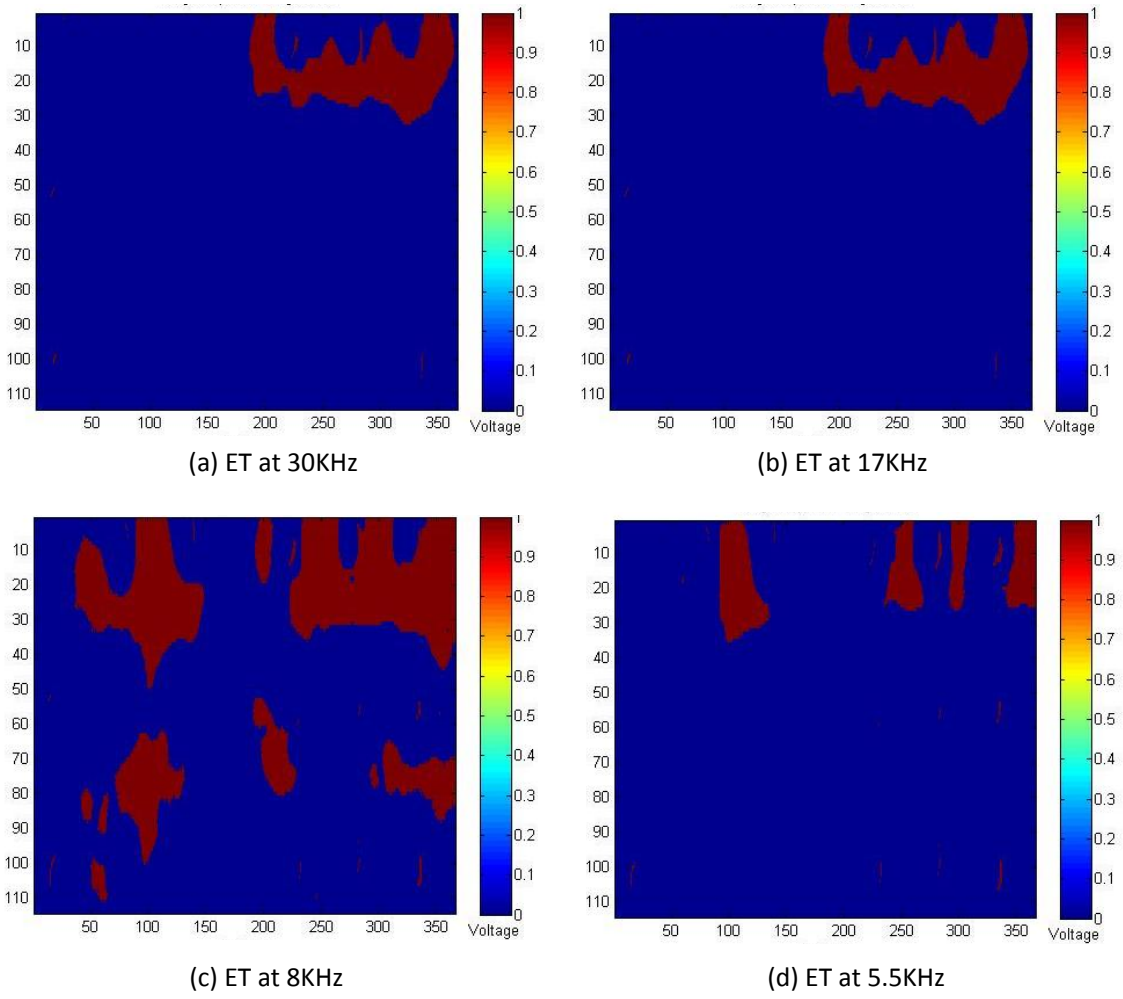

(a) ET at 30KHz

(b) ET at 17KHz

(c) ET at 8KHz

(d) ET at 5.5KHz

Figure 5-4 Adaptive Thresholding of Eddy Current Measurements

To quantify the thickness loss due to of corrosion, data fusion is applied by using Equations (17) and (18). Setting m=3, the window of first 12 elements generated the first fusion result. After each result the window moves right till all the fusion results are calculated. The final spatial frequency data fusion of multi frequency measurement system was obtained through the

multiplication of normalized weights with actual spatial frequency matrix as shown in Figure 5-5.

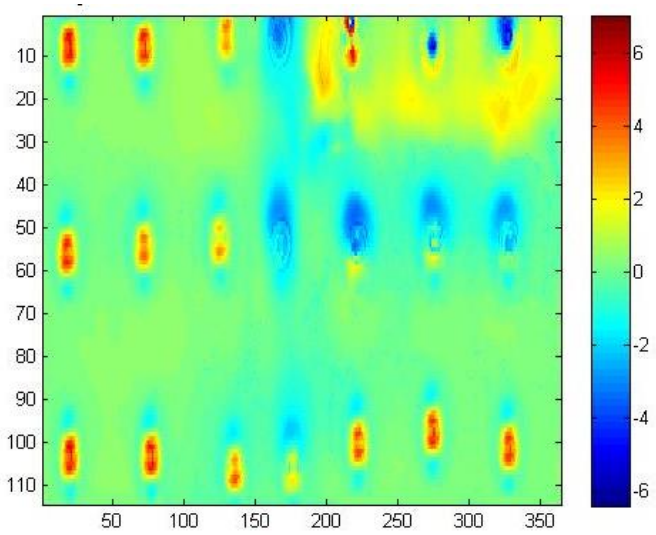

Figure 5-5 Data Fusion Result

The adaptive thresholding scheme is also applied on fused image and results are then compared with actual x-ray thickness mapping to evaluate the proficiency of the proposed technique. In Figure 5-6 (a), the pixel levels in yellow represent the thickness loss area except the rivets. The adaptive thresholding is also applied on the fused eddy current data as shown in. Figure 5-6 (b).

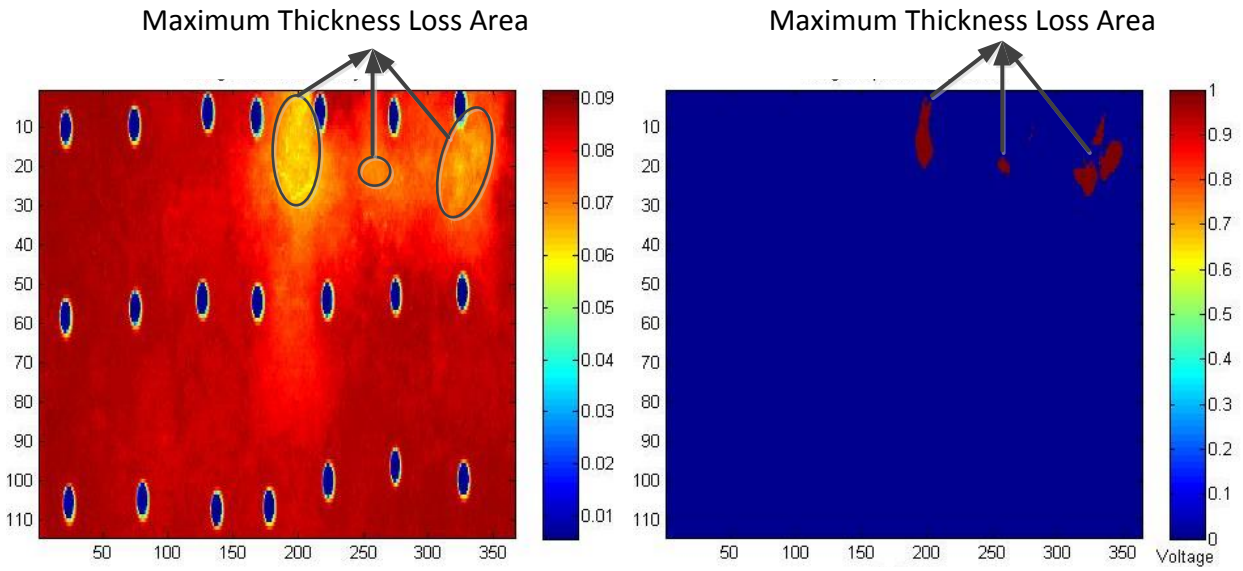

(a) Actual X-Ray Thickness Mapping

(b) Adaptive Thresholding of Fused Image

Figure 5-6 Corrosion Quantification Result

5.4 Discussion

The proposed data fusion technique for multi-frequency eddy current data will also be applied on other eddy current testing applications. The spatial frequency correlation based data fusion method paper offers accurate and precise detection of thickness results than the results achieved using single frequency measurement data. The entire red portion (without thickness loss) in the fused image is vanished and thickness loss areas are visible in adaptive thresholded image as shown in Figure 5-6 (b). As shown in Figure 5-4, the thickness loss areas are not accurately detected using single frequency measurement modes.

The method fully integrates the relationship between spatial data points and frequency information of multi frequency ET measurements. The method also considers the consistency and stability at each frequency to make fusion result more reasonable

CHAPTER 6

6 CONCLUSION

A novel flaw classification and profiling algorithms was developed using data fusion of multifrequency eddy current measurements for defect identification and characterization in aircrafts structures. The results presented in this thesis indicate that these algorithms are capable of accurately solving flaw detection with a relatively low computational effort, even in the presence of noise.

The results obtained with the GRNN approach for depth profiling also indicate that this approach can provide a measure of confidence in its prediction. This feature is especially useful when the inversion process must be performed in the presence of noise.

In the last, novel spatial frequency correlation method for data fusion has been proposed to enhance the accuracy and stability of multi frequency eddy current measurement system. The method was applied to multi-frequency eddy current measurements of aging aircraft structure. The promising result indicates the efficacy of the technique.

CHAPTER 7

7 FUTURE WORK

Future work can include the designing a generic algorithm that would detect and classify all possible types of defect without any user intervention.

Development of confidence measures for classification and flaw profiling. These measures will provide additional information for the analyst to determine the level of confidence of the algorithms in its decisions.

REFRENCES

1. Non Destructive Testing Handbook, second edition: Volume 10, Non Destructive Testing Overview. Columbus, OH: American Society for Non Destructive Testing (1996)
2. Non Destructive Testing Methods. TO33B-1-1 (NAVAIR 01-1A-16) TM43-0103. Washington DC: Department of Defense (June 1984)
3. Janousek, L.; Capova, K.; Yusa, N.; Miya, K. Multiprobe inspection for enhancing sizing ability in eddy current nondestructive testing. IEEE Trans. Magn. 2008, 44, 1618-1621.
4. R.C. McMaster S.A.W., A Basic Guide for Management Choice of non Destructive Test, in Symposium on the role of Non Destructive Material Testing in the Economics of Production. A. International, Editor. 1951: West Conshohocken.
5. Saxby, S.M., Magnetic Testing of Iron. Engineering, 1886. 5: p. 279.
6. Forster, F., The First Picture: A Review of the initial steps in the development of Eight Branches of Non Destructive Material Testing Materials Evaluation, 1983. 41(3): p. 1477-1488.
7. Burrows, C.W., Apparatus for Testing Magnetizable Objects. 1928: United States.
8. Libby, H.L., Introduction to Electromagnetic Nondestructive Test Methods, 1971, New York: Jhon Wiley and Sons.
9. T. Khan, P. Ramuhali, Particle filter based multi-sensor fusion for solving low frequency electromagnetic NDE inverse problems, IEEE Trans. Of Measurement and Instrumentation Vol: 60 No:6, June 2011, pp. 2142-2153.
10. G. Yang, T . Khan, L. Udpa, S. Udpa, J. Kim, Pre-processing methods for eddy current data analysis using Hilbert-Huang Transform, to be presented at 15th international symposium on electromagnetic and mechanics, Italy, Sep 2011.

11. D.S. Forsyth et al, The role of data fusion in NDE for aging aircraft, Proc, SPIE, vol. 3394, (2000) pp.47-58.
12. Corrosion Detection Technologies
13. G. Yang, T . Khan, L. Udpa, S. Udpa, J. Kim, Pre-processing methods for eddy current data analysis using Hilbert-Huang Transform, to be presented at 15th international symposium on electromagnetic and mechanics, Italy, Sep 2011.
14. D.S. Forsyth et al, The role of data fusion in NDE for aging aircraft, Proc, SPIE, vol. 3394, (2000) pp.47-58.
15. J. S. Knoop, J. C . Aldrin, Fundamental Feature Extraction Methods for the Analysis of Eddy Current Data, Airforce Research Laboratory, December 2006, USA.
16. Y. Sun, X. Lou, H. Liu, Multi-sensor Data Fusion Method Based on Twice Spatial-temporal Correlation, Journal of Computational Information Systems, 2012, 655-663
17. S. Tang, X. Li, Application of spatial temporal correlation in data fusion for wireless sensors network, Conference Anthology, IEEE, 2013, 1-5.
18. J. Chen, Q. Ji, Online spatial temporal data fusion for robust adaptive tracking, IEEE, 2007
19. Spatio temporal correlation and visual signaling in a complete neuronal population
20. H. J. Helze, G.R Mangun, Combined spatial and temporal imaging of brain activity during visual selective attention in humans, Letters to Nature, Vol 372, 1994.
21. T. Khan, P. Ramuhali, Particle filterbased multi-sensor fusion for solving low frequency electromagnetic NDE inverse problems, IEEE Trans. Of Measurement and Instrumentation Vol: 60 No:6, June 2011, pp. 2142-2153.

22. T. Khan, P. Ramuhalli, Sequential Monte Carlo Based Data Fusion For Characterization Of Corrosion On Aging Aircraft Structures, Electromagnetic Nondestructive Evaluation, 2010, 181-188.
23. S. Thirunavukkarasu, B. P. C. Rao, A. K . Soni, Comparative performance of image fusion methodologies in eddy current testing, Research Journal of Applied Sciences, 2012, 5548-5551.
24. Z. Liu, D. Forsyth, A Data-Fusion Scheme for Quantitative Image Analysis by Using Locally Weighted Regression and Dempster–Shafer Theory, IEEE Transaction of Instruments and Measurements, Vol 57, 2008.